Control of Cascaded DC – DC Converter Based Hybrid Battery Energy Storage Systems – Part I: Stability Issue

Nilanjan Mukherjee, *Member, IEEE* and Dani Strickland

***Abstract*- There is an emerging application which uses a mixture of batteries within an energy storage system. These hybrid battery solutions may contain different battery types. A dc-side cascaded boost converters along with a module based distributed power sharing strategy has been proposed to cope with variations in battery parameters such as, state-of-charge and/or capacity. This power sharing strategy distributes the total power among the different battery modules according to these battery parameters. Each module controller consists of an outer voltage loop with an inner current loop where the desired control reference for each control loop needs to be dynamically varied according to battery parameters to undertake this sharing. As a result, the designed control bandwidth or stability margin of each module control loop may vary in a wide range which can cause a stability problem within the cascaded converter. This paper reports such a unique issue and thoroughly investigates the stability of the modular converter under the distributed sharing scheme. The paper shows that a cascaded PI control loop approach cannot guarantee the system stability throughout the operating conditions. A detailed analysis of the stability issue and the limitations of the conventional approach are highlighted. Finally in-depth experimental results are presented to prove the stability using a hybrid battery energy storage system prototype.**

***Index Terms*—cascaded DC-DC converters, hybrid battery energy storage systems, stability**

NOMENCLATURE

ω_i	Weighting factor for i^{th} module current	
$V_{batt,i}$	Steady state battery voltage of i^{th} module	V
$v_{batt,i}$	Instantaneous battery voltage of i^{th} module	V
$i_{batt,i}$	Instantaneous current of i^{th} battery module	A
$I_{batt,i}$	Steady state current of i^{th} battery module	A
$v_{dc,i}$	Instantaneous capacitor voltage of i^{th} module	V
$V_{dc,i}$	Steady state module dc-link voltage of i^{th} module	V
V_{dc}	Steady state total DC-link capacitor voltage	V
v_{dc}	Instantaneous inverter dc-link capacitor voltage	V
I_{dc}	Steady state common DC-link current	A
i_{dc}	Instantaneous common DC-link current	A
d_i	Instantaneous duty cycle of i^{th} boost converter module	
D_i	Average duty cycle of i^{th} boost converter	

Manuscript received January 20, 2015; revised April 29, 2015, August 14, 2015 and September 09, 2015; accepted October 30, 2015.

N. Mukherjee is with the school of electronic, electrical and systems engineering at the University of Birmingham, Birmingham, B15 2SA, UK. (Email: n.mukherjee@bham.ac.uk) and D.Strickland is with the power electronics and power systems group at Aston University, Birmingham, B4 7ET, U.K. (Email: D.STRICKLAND@aston.ac.uk)

I. INTRODUCTION

EX-TRANSPORTATION batteries for grid support applications are gaining increased research attention as the number of electric vehicles on the road increases. There are reports of projects both in industry [1]– [2] and academia [3]–[6] covering both theoretical studies and small prototype units with similar batteries. However, battery chemistry development is a highly funded research area and it is unlikely that battery chemistry in vehicles to date will be the same as that in 10 years' time. In addition to changes in chemistry, battery sizes are continuous adapting to meet the requirements of the vehicles. Therefore, one of the major challenges of a second life battery energy storage system is to make sure it is not tied to any one chemistry or module size but can integrate different types of batteries with different characteristics into a grid connected converter as reported in [4].

To integrate hybrid batteries into a system requires a modular approach utilizing battery modules with sets of series connected cells per module. Unfortunately, from a reliability perspective the greater the number of series connected cells, the lower the module reliability [5]. Therefore, low number of series connected cells within a module is a preferred approach. There are two main forms of modular DC-DC converters which can integrate these low voltage batteries (e.g. <100V) to a grid-tie inverter: a) a parallel converter approach and b) a series/cascaded approach. A previous study on this area suggested a cascaded approach over the parallel approach from reliability and cost perspective [6]. Apart from the reliability/cost issues, the parallel approach has other drawbacks in conjunction with low voltage energy sources [7], [8] such as: a) low converter efficiency (e.g. < 90%) due to the extremely high step-up ratio (10 – 20) required to meet the full dc-link voltage of the inverter, b) increased high frequency current ripple on the inductor and on the battery side, c) reduced switch utilisation, d) greater effect on control coming from the system parasitic at a high converter duty ratio and e) increased the size and cost of the overall converter to attain a high efficiency. For these reasons, this paper adopts a series connected DC-DC topology.

However, a conventional cascaded boost converter structure is not fault-tolerant in nature which is unable to bypass a faulty battery module. Therefore, this study uses an H-Bridge configuration to allow each module to handle unexpected battery failure as shown in Fig. 1. Under normal condition only the top switch of the network conducts (T_i) and under abnormal conditions, the bottom device (T_{ii}) conducts to isolate the fault battery module. Due to the presence of different types of batteries in the system, a module based distributed power sharing strategy based on a weighting function has been presented [9]. The weighting function concept is to distribute the total power among the different battery modules according to their instantaneous battery parameters so that they aim to charge/discharge together within a charge/discharge cycle. This avoids the cross-balancing between the cells during a cycle and the energy from the battery cells are supplied or absorbed in a uniform manner. To undertake the weighting function control, each module needs to be operated to different voltage and current levels with its own control loops as shown in Fig. 2. The desired module voltage or current parameter/reference of the control loop is dynamically varied according to the individual battery parameters such as, state-of-charge/capacity to regulate the module voltage and current according to an appropriate function. The consequence of this type of operation could be the possibility of an overall stability problem which is an important issue for the stable operation of the converter. This issue is discussed in this paper and investigated in detail.

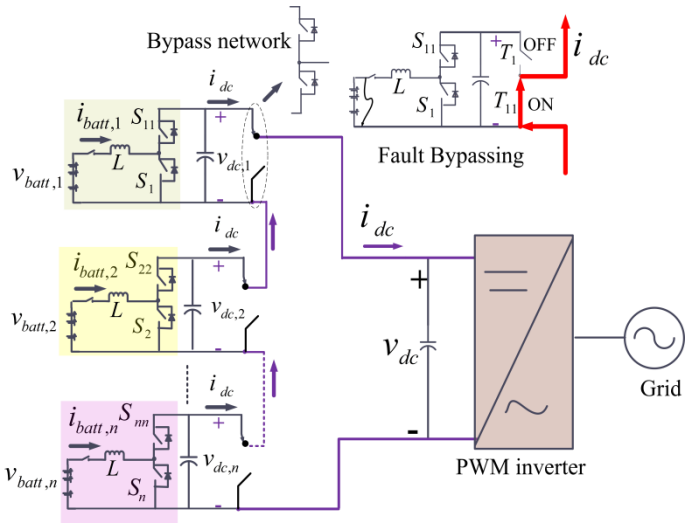

Fig. 1 Fault-tolerant cascaded DC-DC structure to integrate hybrid battery system to the power grid

There are broadly three types of control system and associated stability studies which have been considered in previous research that can be thought of as similar in nature to the present application: a) converters with the same type of sources such as, batteries [10]– [15], super-capacitors or fuel cells [16] – [17], b) converters with different types of sources such as, PV with battery, or wind/PV hybrid energy systems [18] – [21], c) converters with the same type of sources under different operating conditions such as PV panels under partial shading [7] – [8].

In the first case, two types of control studies have reported: a) using non-modular converters in energy storage or renewable energy systems, where the system stability due to a sudden load variation and power demand mismatches have been identified as the main reason for stability, e.g. [10]–[15], b) using modular converters which consists of the same type of sources (batteries/super-capacitors), a module balancing strategy was reported to enhance the overall performance of the system [14] – [15] without concentrating on the stability aspect. Some of the research studies explicitly try to analyse the system stability due to the battery parameter variation using a single battery bank, e.g. in [13]. However, no controller performances under varying parameter conditions, no rigorous stability study and also no experimental validation of the stability issue was demonstrated to justify.

In the second case, energy management strategies using the grid side converter control have been reported [18] – [21]. The power mismatch between the multiple sources produces line side voltage and frequency stability problem depending on the *R/X* ratio of the network. The grid impedance variation was found to be one of the significant reasons for the inverter instability and an adaptive controller was proposed [20], [21]. However, no stability issues have been reported due to the interaction among different sources because these systems operate slowly (e.g. in the order of hundreds of milliseconds). There have been few previous studies which focus on control and stability aspects of modular PV-battery hybrid systems such as, in [22] but it uses parallel converters with a central dc-link to interface with the grid and concentrated in analysing more closely the effect of system dynamics using standard PI controller under various load conditions. Therefore, these are not directly related to the present research work which mainly deals with the cascaded converters.

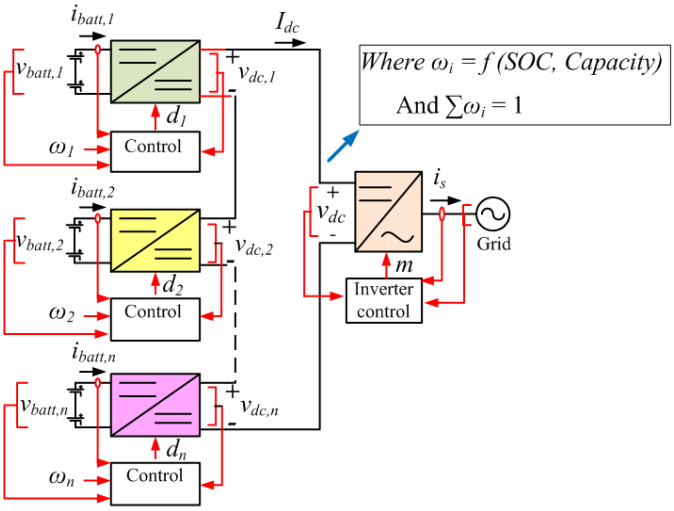

Fig. 2 Schematic of distributed power sharing in hybrid battery application

In the third type of studies, distributed MPPT control of cascaded DC-DC converter based PV systems has been considered. A weighting factor based strategy similar to the present work was reported e.g. in [8]. The weighting factor was solely based on different radiation conditions where the only variable parameter was solar irradiation factor. The module based control was designed by the PI loop using fixed controller parameters and no such stability issue was reported.

There have been previous studies that have reported issues with control stability aspects of modular power converters, e.g. in drive applications where the sub-module capacitor

voltage ripple at a low frequency can create instability within the converter [23], [24].

Apart from these, other research studies presented the stability aspect of single DC-DC buck or boost converters [25] – [27] considering their parasitic effects. Some of the past research activities discussed the operational stability aspects of modular DC-DC converters, e.g. interconnection problem such as, voltage sharing or current sharing issues of input parallel output series (IPOS) or input parallel output parallel (IPOP) based systems [28] – [29]. These studies do not focus on control stability issues but more on the operational stability issues such as, mitigation of circulating current and cross-coupling effects among the modules and are therefore not relevant to the work presented in this paper.

The control stability aspect of a modular energy storage system using cascaded converters due to parameter variations or under distributed power sharing has not been explicitly reported in literature because the existing control system in modular converters uses balancing strategies and operates with a fixed voltage/current reference with fixed control parameters where the system stability margin remains within the limit.

This paper reports such an issue and explains why there could be a stability issue when using the cascaded PI control loop per module with fixed control parameters in a full charging/discharging cycle especially using cascaded converters. The stability problem has been analysed first considering the battery state-of-charge/capacity variations both in time and frequency domain and then experimentally validated using a three module based grid connected converter prototype to find how severe the problem could be.

II. CONTROL STRUCTURE

The distributed sharing strategy adopted in this paper of the cascaded DC-DC converter is based on the previously derived method as reported in [9]. Alternative energy management strategies could be employed to generate different weighting functions, but the process employed in this paper to ensure control and stability retains relevance even under different strategies. This previously derived weighting function is dependent on battery capacity, battery voltage limits, battery state of charge and battery impedance (SOH indication) with the following assumptions:

- A battery capacity has been taken as the maximum charge left (Q_{max} in C or Ah) that a battery can deliver to a load.
- Instantaneous charge left within a battery module is taken as the product of state-of-charge (*SOC*) and Q_{max}.
- Open circuit voltage (*OCV*) = $v_{batt,i} \pm i_{batt,i}\, Z_i$ where '±' refer to the discharging or charging condition
- *SOC* is a linear function of the battery *OCV*

Charging/discharging depends purely on the module current. Therefore in order to appropriately utilise the hybrid batteries within the same converter, a current sharing strategy among the modules is necessary as reported in [9]. The equation (1) shows the sharing scheme based on weighting factors. Note that the expression of weighting factor is different in charging and discharging. The control system of module based distributed power sharing is explained with the help of Fig. 3. The battery voltage, battery current and module dc link voltage are measured and reported to the control system which then generates the switching signals for the power electronic switches (S_1, S_{11}, S_2 etc.). In order to control each module independently in this converter, the desired module voltage references ($v_{dc,1}^*$, $v_{dc,2}^*$ … $v_{dc,n}^*$) are generated according to a battery weighting factor ($\omega_1..\omega_n$) as shown in Fig. 3 which acts to share the battery current according to the desired weighting ratio. This can be derived using the module power balance equation as shown in (1) – (5). η_i is the module efficiency (assumed to be approximately 1). Each voltage reference is the function of its ω_i and $v_{batt,i}$ because v_{dc}^* can be assumed to be constant for a given grid voltage.

$$\frac{i_{batt,1}}{\omega_1} = \frac{i_{batt,2}}{\omega_2} = \cdots = \frac{i_{batt,n}}{\omega_n} \text{ Where} \quad (1)$$

$$\omega_i = \frac{SOC_i\, Q_{max,i}}{\sum_{k=1}^{n} v_{batt,k} SOC_k\, Q_{max,k}}\ discharging,\ \forall i = 1,2,\dots,n$$

$$= \frac{(1-SOC_i)\, Q_{max,i}}{\sum_{k=1}^{n} v_{batt,k}(1-SOC_k)\, Q_{max,k}}\ charging \text{ And } \sum_{i=1}^{n} \omega_i = 1$$

$$v_{dc,i} i_{dc} = \eta_i\, v_{batt,i} i_{batt,i} \quad (2)$$

From the derivation of the weighting function as shown in (1);

$$i_{batt,i}^* = C\omega_i \text{ or } \propto \omega_i \quad \forall i = 1 \dots n \quad (3)$$

From the power balance equation (2) for a constant i_{dc} and η_i

$$v_{dc,i}^* = \frac{\eta_i C v_{batt,i} \omega_i}{i_{dc}} \text{ or } \propto v_{batt,i}\omega_i\ \forall i = 1 \dots n \quad (4)$$

Now, $\sum v_{dc,i}^* = v_{dc}^*$ this gives the following expression;

$$v_{dc,i}^* = v_{dc}^* \frac{\omega_i v_{batt,i}}{\sum_{k=1}^{n} \omega_k v_{batt,k}}\ \forall i = 1 \dots n \quad (5)$$

A. Distributed Voltage Control Structure

Each module consists of two cascaded control loops: a) a slow outer voltage module voltage loop and b) a fast inner current loop. Fig. 4 shows this cascaded control loop structure. The associated inner current loop delay (e^{-sT_d}) has been taken as four times of the sample time (T_s). The open loop transfer function for the voltage control loop can be derived as shown in (6). The control loop parameters K_v and T_v are assumed to be fixed for the purpose study. It can be seen that the open loop transfer function for the module voltage loop $GH_v(s)$ depends $v_{dc,i}$ and $v_{batt,i}$.

$$GH_v(s) = K_v \left(\frac{1+sT_v}{sT_v}\right)\left(\frac{1}{1+sT_d}\right)\left(\frac{v_{batt,i}}{v_{dc,i}}\right)\left(\frac{1}{sC}\right) \quad (6)$$

Now with the help of Fig. 4(a), the following relation between $v_{dc,i}^*$ and $v_{dc,i}$ can be found.

$$\frac{v_{dc,i}}{v_{dc,i}^*} = \frac{GH_v(s)}{1+GH_v(s)} \quad (7)$$

Substituting $v_{dc,i}$ from (7) in (6) gives,

$$GH_v(s) = K_v \left(\frac{1+sT_v}{sT_v}\right)\left(\frac{1}{1+sT_d}\right)\left(\frac{v_{batt,i}}{\frac{GH_v(s)}{1+GH_v(s)} v_{dc,i}^*}\right)\left(\frac{1}{sC}\right) \text{ Or}$$

$$\frac{GH_v^2(s)}{1+GH_v(s)} = K_v\left(\frac{1+sT_v}{sT_v}\right)\left(\frac{1}{1+sT_d}\right)\left(\frac{v_{batt,i}}{v_{dc,i}^*}\right)\left(\frac{1}{sC}\right) \quad (8)$$

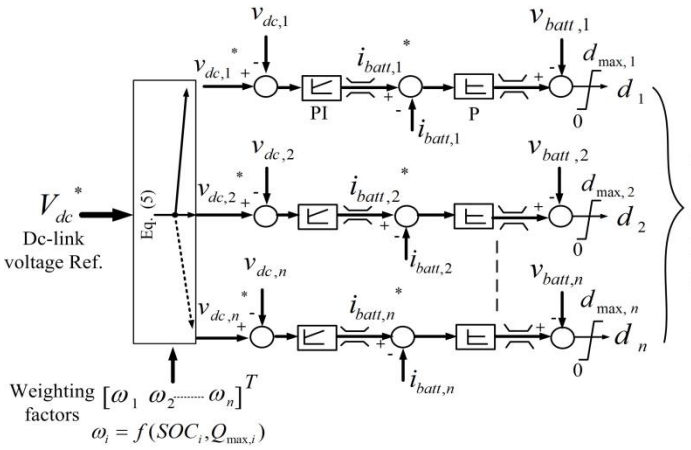

Fig. 3 Distributed voltage based control for cascaded DC-DC converters

Now solving the quadratic equation (8) to find $GH_v(s)$,

$$GH_v(s) = \frac{F(s) \pm \sqrt{F^2(s)+4F(s)}}{2} \text{ Where}$$

$$F(s) = K_v\left(\frac{1+sT_v}{sT_v}\right)\left(\frac{1}{1+sT_d}\right)\left(\frac{v_{batt,i}}{v_{dc,i}^*}\right)\left(\frac{1}{sC}\right) \quad (9)$$

It can be seen that the terms like $v_{batt,i}$ and $v_{dc,i}$ in the transfer functions (6) and (9) are essentially time varying. However, these are slow variables and take several minutes to change depending on the battery charge capacity which is normally 10's Ah. Therefore, it can be treated similar to a time invariant system.

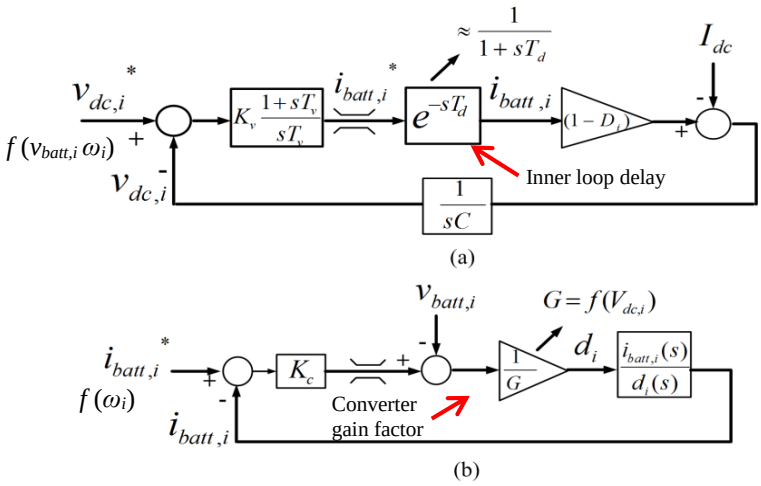

Fig. 4 Control loop modelling per module: a) voltage loop, b) current loop

B. Control Loop Parameter Design

The design of PI controller can be performed using the *symmetric optimum* method [30] pre-defining a certain phase margin (PM). According to this method, the regulator gains K_v and T_v are selected such that the amplitude and the phase plot of $GH_v(s)$ are symmetrical about the crossover frequency ω_{gc}, which is at the geometric mean of the two corner frequencies of $GH_v(s)$. Now, assume $T_v = aT_d$, where 'a' is a nonnegative real value, therefore, expressions of gain-cross over frequency ω_{gc} and PM become the following:

$$\omega_{gc,i} = \frac{1}{\sqrt{(T_vT_d)}} = \frac{1}{aT_d} \quad (10)$$

$$PM = \tan^{-1}\frac{\omega_{gc,i}(T_v - T_d)}{1+\omega_{gc,i}^2 T_vT_d} = \tan^{-1}\left\{\frac{1}{2}\left(a-\frac{1}{a}\right)\right\} \quad (11)$$

$$K_{v,i} = \frac{1}{a}\left(\frac{V_{dc,i}{}^d}{V_{batt,i}{}^d}\right)\frac{1}{T_d}C \text{ and } T_v = a^2T_d \quad (12)$$

Where $V_{dc,i}{}^d$ and $V_{batt,i}{}^d$ are nominal values of $v_{dc,i}$ and $v_{batt,i}$. For a 12V battery if we assume $V_{batt,i}{}^d$ = 12V, $V_{dc,i}{}^d$ = 50V (< V_{dc}), C = 2200μF, T_d = 4×100μs and the desired PM = 70°, this gives a = 6 and k_v = 3.8 and T_v = 14.4ms.

III. Parameter Variation and Stability Issue

Through the formulation of $v_{dc,i}^*$ it can be seen that two different input variables directly affect the weighting function and the converter stability: a) SOC_i and b) capacity $Q_{max,i}$. These variables impact stability through (6) to (9) where a variation of ω_i causes $v_{dc,i}^*$ to change which consequently changes the open loop gain of $F(s)$ as it sits in the denominator in (9). In other words, any change in $v_{dc,i}^*$ also changes $v_{dc,i}$ and it causes the open loop gain of $GH_v(s)$ ($=K_v\frac{v_{batt,i}}{v_{dc,i}}$) to vary according to (6) which in turn alters the designed gain crossover frequency or the closed loop bandwidth. The expressions for gain crossover frequency can be found by solving (13). The phase margin (PM) is derived in (14) which depends on $\omega_{gc,i}$, T_v and T_d. However, for a fixed set of T_v and T_d, (which can be assumed to be fixed for a system) the PM is mainly governed by $\omega_{gc,i}$. Due to the presence of a higher order equation, an explicit expression is difficult to find from (13). Therefore, frequency response plots have been used to analyse the effect of variation of phase margin and gain crossover frequency in sub section (IIIA).

Since the parameters like *SOC*, $v_{batt,i}$ etc. are time varying, bode plots cannot be shown on an continuous basis. Therefore, in order to visualise the trend of gain crossover frequency and phase margin variation over a cycle, frequency plots have been shown at discrete instances, e.g. at *SOC* = 10%, 50% or at *SOC* = 90% etc. Note: the rate of variation of the open loop controller gains e.g. $K_v\frac{v_{batt,i}}{v_{dc,i}}$ is different in charging and discharging. Therefore, the variations of the controller gain both in charging and discharging mode have been presented to identify the differences.

A. Open loop Gain Variation

This section analyses the variation of the effective controller gain $K_{v,i}\frac{v_{batt,i}}{v_{dc,i}}$ in (6) to understand the stability. This variation could be different for the different battery modules within the same converter because the weighting factor (ω_i) variation causes some of the $v_{dc,i}$ to increase and some of them to decrease in order to keep the sum ($\sum v_{dc,i}$) constant on an instantaneous basis. This is shown in Fig. 5 and Fig. 6 where the variation of the gain has been presented for three different battery types within a discharge and charge cycle. It is interesting to note in this case, the controller gain for a 12V

10Ah battery module varies around 2 – 3 times during discharging mode when the *SOC* varies between 0 – 100%. On the other hand, during charging mode the controller gain for a 7.2V 6.5Ah module shows a wide variation. The gain for the other modules does not vary in the same way. The variation of the controller gain is dependent on the relative variation of $\frac{v_{batt,i}}{v_{dc,i}}$ and which could be different for charging and discharging.

$$\left|GH_v(j\omega_{gc,i})\right| = \frac{K_v}{T_v}\frac{V_{batt,i}}{V_{dc,i}C}\left(\frac{\sqrt{1+(\omega_{gc,i}T_v)^2}}{(\omega_{gc})^2\sqrt{1+(\omega_{gc,i}T_d)^2}}\right) = 1 \qquad (13)$$

$$A\frac{\sqrt{1+xp}}{x\sqrt{1+xq}} = 1 \rightarrow qx^3 + x^2 - A^2xp - A^2 = 0 \quad \text{Where}$$

$$x = {\omega_{gc,i}}^2, A = \frac{K_v}{T_v}\frac{v_{batt,i}}{v_{dc,i}C}, p = {T_v}^2, q = {T_d}^2$$

$$PM = tan^{-1}\frac{\omega_{gc,i}(T_v - T_d)}{1+{\omega_{gc,i}}^2T_vT_d} = f(\omega_{gc,i}) \qquad (14)$$

The inner current loop is designed based on a proportional controller shown in Fig. 4(b). This is done to enhance the stability and dynamic performance. The transfer function is shown in (15). Generally, the inner current loop bandwidth is set to several times higher (typically 20-50 times) than the outer voltage loop for a stable operation.

$$GH_I(s) = K_{c,i}\frac{1}{G}\frac{I_{batt,i}}{(1-D_i)}\frac{1+s\frac{V_{dc,i}C}{(1-D_i)I_{batt,i}}}{1+s^2\frac{LC}{(1-D_i)^2}} \qquad (15)$$

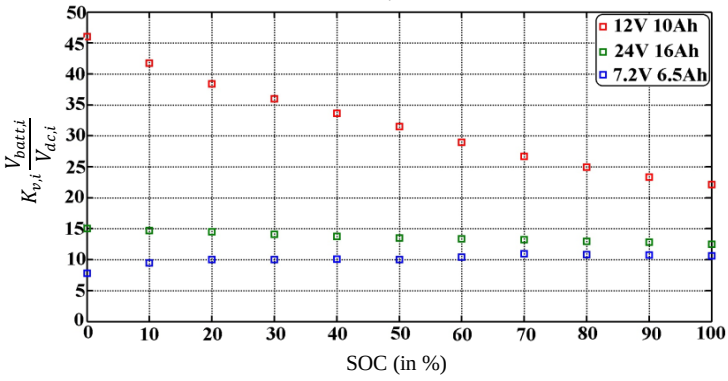

Fig. 5 Variation of the gain $\boldsymbol{K_{v,i}}\frac{V_{batt,i}}{V_{dc,i}}$ within a full discharge cycle

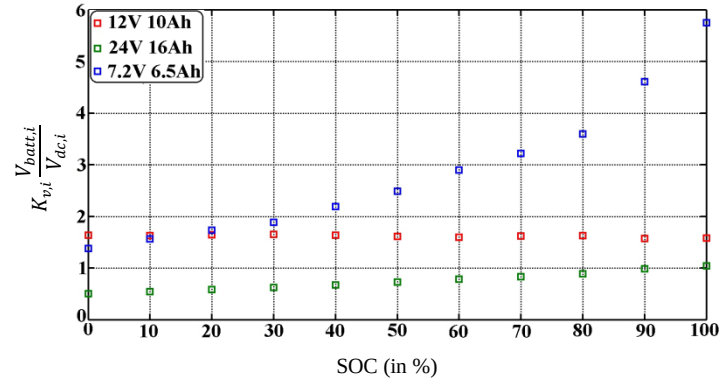

Fig. 6 Variation of the gain $\boldsymbol{K_{v,i}}\frac{V_{batt,i}}{V_{dc,i}}$ within a full charge cycle

Therefore, the high frequency behaviour of the inner loop is more important than its low frequency behaviour. The inner current loop bandwidth can be derived by approximating the transfer function at the high frequency as shown in (16). The term '*G*' depends on the carrier peak. In most cases, a fixed carrier gain can be considered and set to the maximum possible $V_{dc,i}$. However, it is also possible to vary the carrier gain dynamically (i.e. modulated carrier gain). The inner loop performance would be different in these two cases. Both the cases are studied to understand how the inner loop bandwidth varies with ω_i. That is; a) $V_{dc,i}/G$ is nearly constant using a modulated carrier, b) $V_{dc,i}/G$ is variable using a fixed carrier.

$$GH_I(s)\big|_{\omega\to\infty} \approx \frac{K_{c,i}}{sL}\frac{1}{G}V_{dc,i}$$

$$BW = \frac{K_{c,i}}{L} \leftarrow \text{Variable gain carrier and}$$

$$BW = \frac{K_{c,i}}{L}\frac{1}{G}V_{dc,i} \leftarrow \text{Fixed gain carrier} \qquad (16)$$

B. Case Studies: Effect on Stability

State-of-charge (SOC) Variation: *SOC* can be any value between the maximum and minimum limits within a charge/discharge cycle. Therefore, a very low *SOC* at the start or during the transition from charging to discharging or vice-versa can cause decrease of ω_i (according to (5)) which in turn decreases $v_{dc,i}^*$ and $v_{dc,i}$. This variation changes the designed closed loop bandwidth $\omega_{gc,i}$. To understand the effect of such variation on the control loops, frequency domain bode plots are used as shown in Fig. 7 to Fig. 9. It can be seen from Fig. 7 that the gain crossover frequency ($\omega_{gc,i}$) of the outer voltage loop of the 12V module gradually increases with the module *SOC* during discharging mode. In the present case, it changes from 16Hz to 600Hz when the *SOC* varies from 70% to 10%.

It is because the effective controller gain varies in a wide range as depicted in Fig. 5. Note the frequency plot initially crosses the 0dB axis at – 20dB/decade but gradually the slope changes to – 40dB/decade. The stability margin will be different in charging mode but the shape of the frequency plots will show the similar change. The corresponding effect on the inner current loop has been investigated in two stages: a) using a fixed carrier based scheme and b) a variable carrier based scheme from (16). Fig. 8 illustrates the effect on the high frequency bandwidth (BW) of the inner current loop when using a fixed carrier gain (*G*). It can be noted from Fig. 8(b) and Fig. 8(c) that the variation of *SOC* causes the inner loop bandwidth of module – 1 to vary, effectively slowing down the corresponding inner current loop. In the present case, the inner loop bandwidth of module – 1 varies from 2 kHz to 1.2 kHz when the module SOC varies from 70% to 10%. Fig. 9 shows a similar effect on the inner loop using the modulated carrier (variable *G*). Note that the bandwidth of the current loop remains almost unaffected using modulated carriers as expected from the expression (16).

However, in both cases, the ratio of outer to inner loop bandwidth ($BW_{v,i}/BW_{c,i}$) reduces gradually. This becomes more critical when using a fixed carrier gain because the outer loop bandwidth gradually goes up while the inner loop starts to slow down. Fig. 10 and Fig. 11 shows this effect by plotting the ratio of inner loop bandwidth to outer loop bandwidth using all three battery types. The relative

bandwidth stays high at the lower *SOC* during charging and vice-versa during discharging. However, the ratio comes down gradually which can create a stability problem in the cascaded control loop. The variation of the phase margin (PM) with *SOC* is shown in Fig. 12 and Fig. 13 for discharging and charging respectively. It is worth to notice that the PM for some of modules, e.g. 12V during discharging and 7.2V module during charging gradually reduces with the *SOC* during discharging and vice-versa during charging because of the increase of their respective controller gain.

Capacity or $Q_{max,i}$ Variation: The variation of the battery available capacity is another phenomenon in this application where the battery capacity can degrade significantly. The variation of $Q_{max,i}$ can also cause weighting factor ω_i to vary in a wide range. This can also cause similar variation of gain crossover frequency or phase margin.

However, the effect can be considered to be less significant than *SOC* variation because the maximum available capacity is likely to be a slower variable than the *SOC* for a battery. However, there could be a cumulative effect of both low *SOC* along with capacity fade which means a low $Q_{max,i}$ SOC_i in (1).

Therefore, it is difficult to ensure the converter stability with fixed control parameters. The root locus plot can be used to understand the movement of the system loop poles due this variation It is shown for two types of battery systems in two stages: a) for a high state-of-charge (SOC), e.g. 80% during discharging as shown in Fig. 14 and b) for a low state-of-charge (SOC), e.g. 10% as shown in Fig. 15. It can be observed that the root-locus moves from the real axis towards the imaginary axis as the *SOC* reduces during discharging mode. The root-locus tries to align with the imaginary axis. Similar variation can be observed during charging condition mode. Such movement of the system root-locus towards the imaginary axis adversely affects the overall stability and can cause oscillation within the converter.

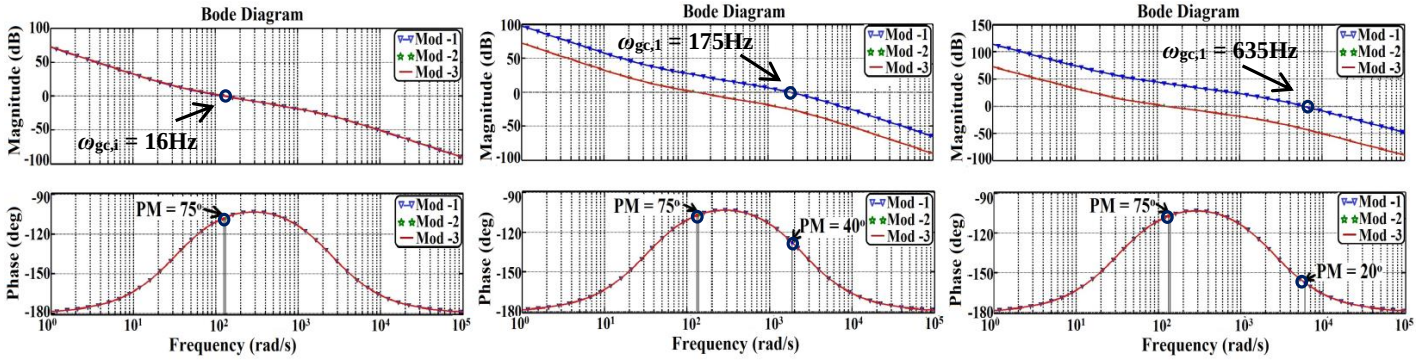

(a) (b) (c)

Fig. 7 An example effect of SOC variation on outer voltage loop for a 12V, 10Ah module during discharging: a) *SOC* = 70%, b) *SOC* = 33%, c) *SOC* = 10%

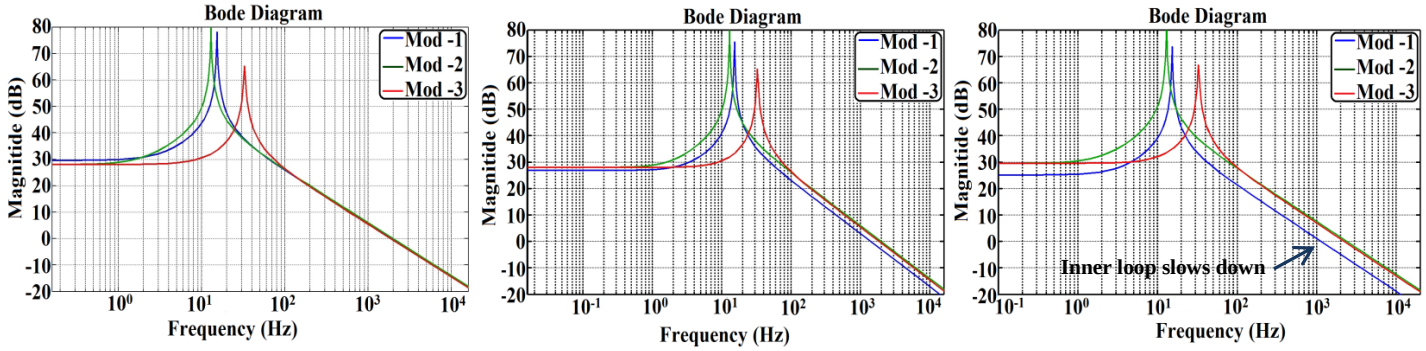

(a) (b) (c)

Fig. 8 Effect of SOC variation on inner loop using fixed carrier gain for a 12V, 10Ah module during discharging: a) SOC = 70%, b) *SOC* = 33%, c) *SOC* = 10%

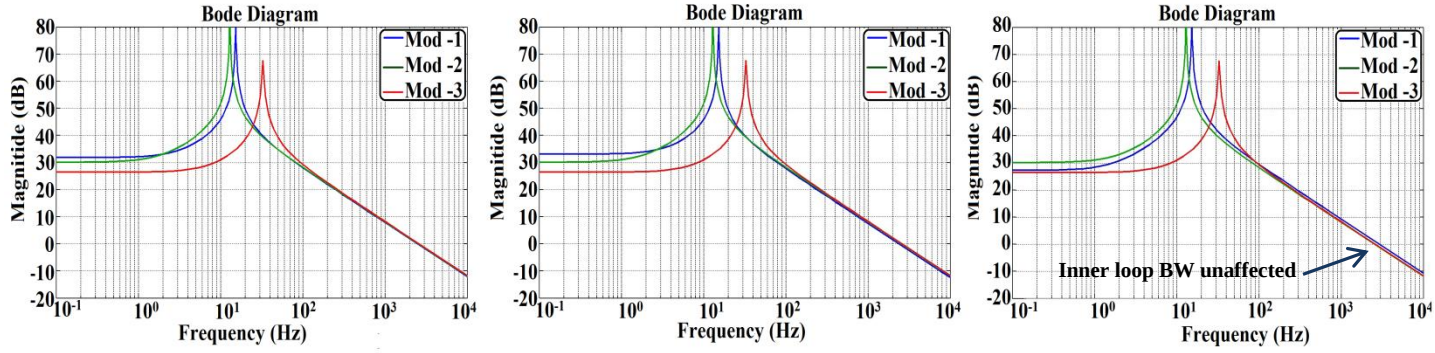

(a) (b) (c)

Fig. 9 Effect of SOC variation on inner loop using modulated carrier gain for a 12V, 10Ah module during discharging: a) *SOC* = 70%, b) *SOC* = 33.3%, c) *SOC* = 10%

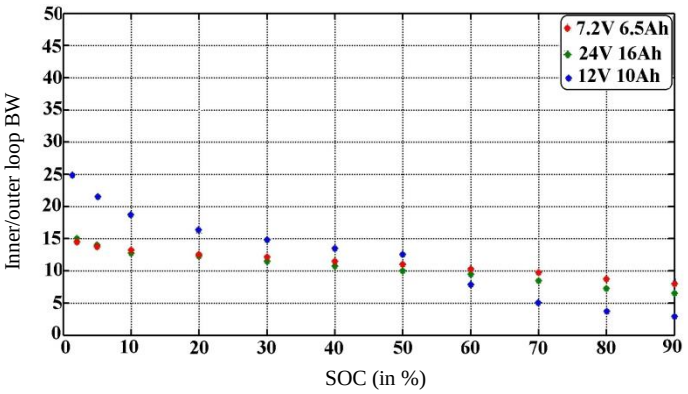

Fig. 10 An example variation of inner to outer loop bandwidth with SOC: discharging

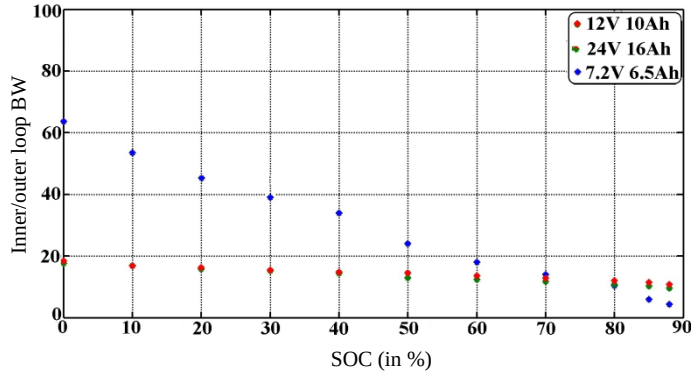

Fig. 11 An example variation of inner/outer loop bandwidth with SOC: charging

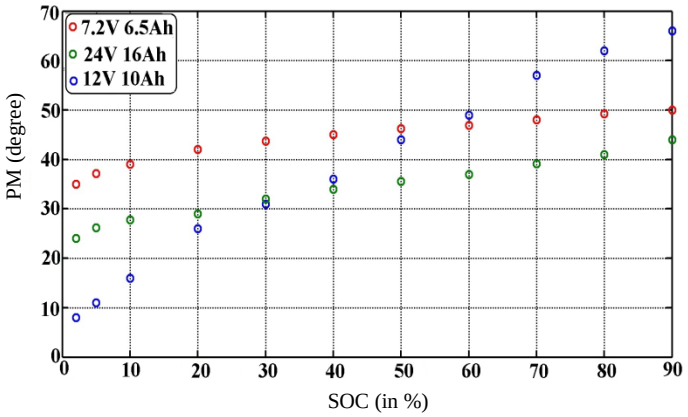

Fig. 12 Variation of stability margin with battery *SOC:* discharging

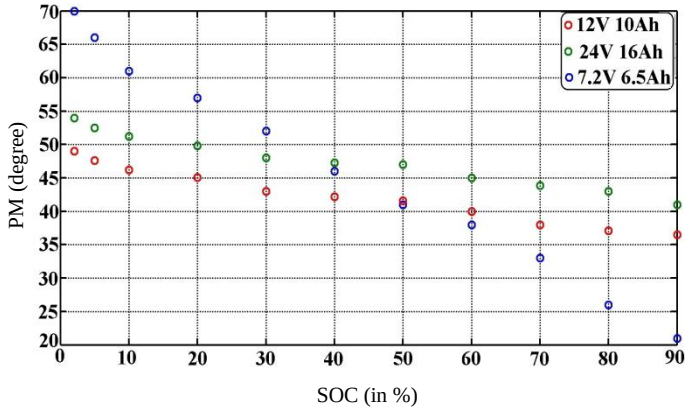

Fig. 13 Variation of stability margin with battery *SOC:* charging

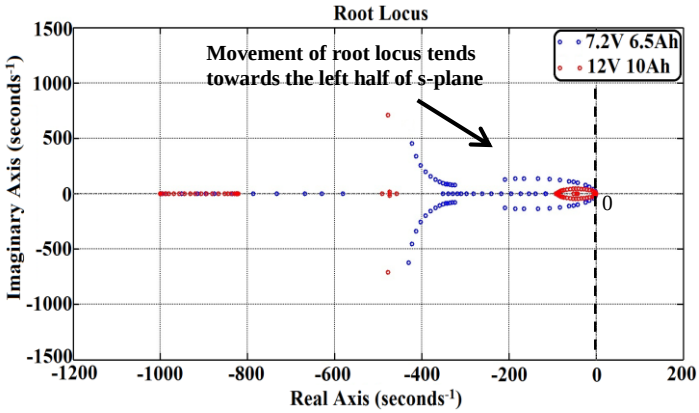

Fig. 14 Variation of closed loop poles for two battery types at SOC = 80%

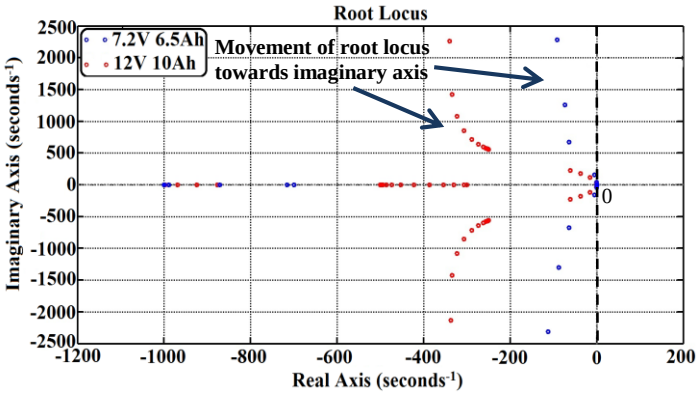

Fig. 15 Variation of closed loop poles for two battery types at SOC = 10%

C. *Interaction between the Modules*

Moreover, if one module becomes oscillatory the stability of the remaining modules also gets adversely affected in this converter. This is because the overall control of the modular DC-DC converter maintains the total dc-link voltage ($\sum v_{dc,i} = v_{dc}$) fixed on an instantaneous basis. Therefore, if one of the voltages ($v_{dc,i}$) gets oscillatory that oscillation propagates in the remaining voltages because the sum of these voltages is constant. This oscillation forces the remaining module currents to be oscillatory because the current reference of each module is the output of corresponding voltage controller as shown in Fig. 3.

IV. EXPERIMENTAL VALIDATION OF THE STABILITY ISSUE

Three different battery types were used in the experimental implementation to prove the stability problem: Module – 1: 12V, 10Ah lead acid (OCV_{max} = 13.8V OCV_{min} = 9.6V) Module – 2: 24V, 16Ah lead acid (OCV_{max} = 27V OCV_{min} = 18V), Module – 3: 7.2V, 6.5Ah NiMH (OCV_{max} = 8.5V OCV_{min} = 5.5V). The overall dc-bus (V_{dc}) of the inverter was controlled to 150V which is then connected to 120V, 50Hz 1-ϕ grid at a 500W power level through Variac in the laboratory.

Case – 1: Fixed carrier gain (G): The converter was run using a fixed set of controller parameters with a fixed carrier gain *G* as explained in section III. Two of the modules were started from a low initial *SOC* during discharging mode and from a high initial SOC during charging mode. These were; module – 3 $SOC_{o,3}$ = 8.4% during discharging, $SOC_{o,3}$ = 90% during

charging and module – 1 $SOC_{o,1}$ = 6.6% during discharging $SOC_{o,1}$ = 92% during charging mode.

The oscillations in battery current due to loss of stability were captured on a LeCroy scope and are shown in Fig. 16 and Fig. 17 for charging and discharging respectively. The module current responses were captured at the moment of connecting to the grid. The currents tend to oscillate between the positive and negative controller limits. It can be seen that all the modules are affected. However, severity depends on the individual control performances.

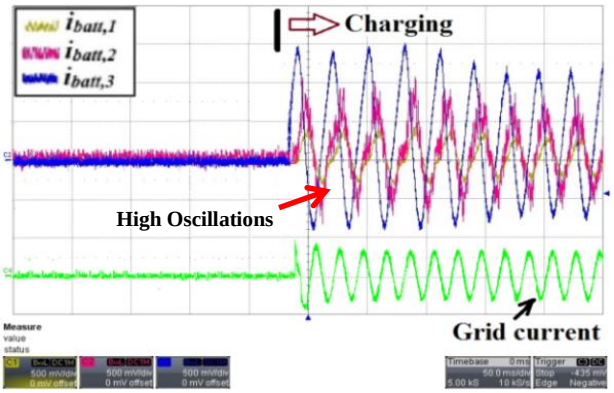

Fig. 16 Fixed PI-controller in charging: scale 50ms/div, grid current 10A/div, module currents 5A/div

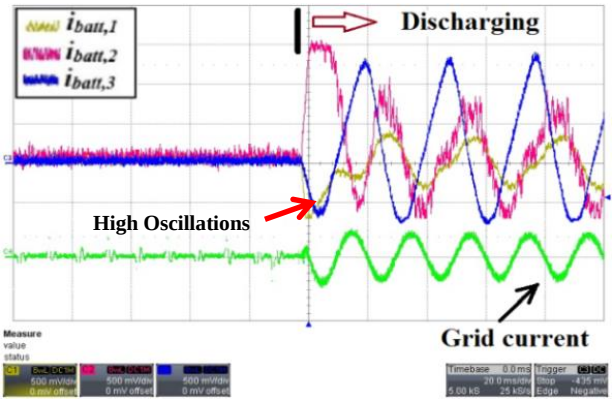

Fig. 17 Fixed PI-controller in discharging: scale 20ms/div, grid current 10A/div, module currents 5A/div

Case – 2: Variable carrier gain (G): Fig. 18 shows the controller response using variable gains as explained in section III. Module current responses are found to be better than the previous case because the inner loop bandwidth remains fixed in this case. However, the problem is totally not eliminated.

Moreover, the stability problem can arise gradually because the state-of-charge (*SOC*) and/or capacity are subjected to change. To demonstrate this, Fig. 19 shows the converter being operated in charging mode over a longer time period using a fixed set of control parameters. It can be observed that the converter was stable but the module currents start to get oscillatory after the point in time shown by the dashed black line which corresponds to the battery modules get close to fully charged. These results show the stability issue occurring in the cascaded converter because of gradual battery parameter variations.

This type of oscillation between the positive and negative controller limits can cause inadvertent tripping of the converter leading to complete shutdown at any time and may impact the converter and also the battery life. Therefore, it is not recommended to operate this converter with fixed controller parameters when the system parameters vary with the time.

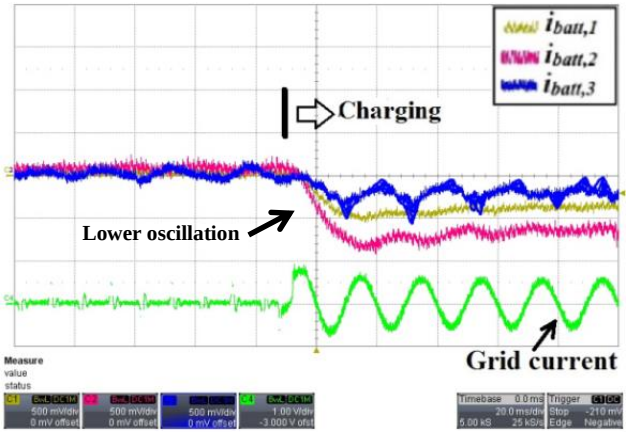

Fig. 18 Variable carrier gain in fixed PI controller during charging: scale time 20ms/div, module current 5A/div, grid current 10A/div

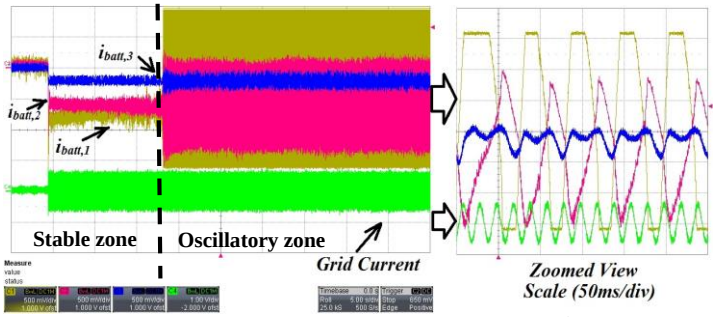

Fig. 19 Gradual instability during charging condition using fixed PI controller: scale time 5s/div, module current 5A/div, grid current 10A/div

V. Conclusion

This paper reports a unique stability issue in the control structure of a cascaded DC-DC boost converter based hybrid battery application under the distributed power sharing. It was found that the variation of state-of-charge and capacity in different battery types could give rise to control stability problem at a module level and at the system level when using the conventional cascaded PI control loop approach with fixed controller parameters. The analysis shows that the problem becomes more severe near the end of charging/discharging cycle and the module currents become highly oscillatory under such operating conditions which can cause inadvertent tripping within the converter and also adversely affect the overall system performance and battery life. The paper shows that the stability of the overall converter is limited by the stability margin of one converter module because of the cascaded structure. This stability issue was explicitly explained and validated experimentally under grid connected conditions. The experimental study shows a good agreement with the theory. The follow-on research will be presented to mitigate this problem using more advanced control methods.

ACKNOWLEDGEMENTS

Authors would like to thank the Engineering and Physical Sciences Research Council (EPSRC), U.K., Grant numbers EP/1008764/1 and EP/137649 for the financial support and the battery manufacturer Altairnano and Opal-rt Europe for their Equipment in experimental validations.

REFERENCES

[1] http://www.abb.com/cawp/seitp202/d3e2f486303c1d47c12577a500479955.aspx [online], accessed Nov. 25, 2015.

[2] http://www.navigantresearch.com/research/second-life-batteries-from-pevs-to-stationary-applications [online], accessed Nov. 25, 2015

[3] Strickland, D.; Chittock, L.; Stone, D.A.; Foster, M.P.; Price, B., "Estimation of Transportation Battery Second Life for Use in Electricity Grid Systems," *IEEE Trans. Sustain. Energy*, vol. 5, no.3, pp.795-803, July 2014.

[4] Mukherjee, N.; Strickland, D., "Control of Second-Life Hybrid Battery Energy Storage System Based on Modular Boost-Multilevel Buck Converter," *IEEE Trans. Ind. Electron.*, vol.62, no.2, pp.1034-1046, Feb. 2015.

[5] Mukherjee, N.; Strickland, D.; Cross, A.; Hung, W., "Reliability estimation of second life battery system power electronic topologies for grid frequency response applications," *in Proc. 6th IET Int. Conf. Power Electronics, Machines and Drives (PEMD 2012)*, vol., no., pp.1,6, 27-29 March 2012.

[6] Mukherjee, N.; Strickland, D., "Second life battery energy storage systems: Converter topology and redundancy selection," *in Proc. 7th IET Int. Conf. Power Electronics, Machines and Drives (PEMD 2014)*, vol., no., pp.1-6, 8-10 April 2014.

[7] Walker, G.R.; Sernia, P.C., "Cascaded DC-DC converter connection of photovoltaic modules," *IEEE Trans. Power Electron.*, vol.19, no.4, pp.1130-1139, July 2004

[8] Bratcu, A.I.; Munteanu, I.; Bacha, S.; Picault, D.; Raison, B., "Cascaded DC–DC Converter Photovoltaic Systems: Power Optimization Issues," *IEEE Trans. Ind. Electron.*, vol.58, no.2, pp.403-411, Feb. 2011.

[9] Mukherjee, N; Strickland, Dani; Varnosfaderani, Mina Abedi, "Adaptive control of hybrid battery energy storage systems under capacity fade," *in Proc. 16th Eur. Conf. on Power Electronics and Applications (EPE'14-ECCE Europe)*, vol., no., pp.1-10, 26-28 Aug. 2014.

[10] Kanchanaharuthai, A.; Chankong, V.; Loparo, K.A., "Transient Stability and Voltage Regulation in Multimachine Power Systems Vis-à-Vis STATCOM and Battery Energy Storage," *IEEE Trans. Power Syst.*, vol.30, no.5, pp.2404-2416, Sept. 2015.

[11] Serban, I.; Teodorescu, R.; Marinescu, C., "Energy storage systems impact on the short-term frequency stability of distributed autonomous microgrids, an analysis using aggregate models," *IET Renew. Power Gener*, vol.7, no.5, pp.531-539, Sept. 2013.

[12] Mithulananthan, N.; Shah, R.; Lee, K.Y., "Small-Disturbance Angle Stability Control With High Penetration of Renewable Generations," *IEEE Trans. Power Syst.*, vol.29, no.3, pp.1463-1472, May 2014

[13] Bazargan, D.; Filizadeh, S.; Gole, A.M., "Stability Analysis of Converter-Connected Battery Energy Storage Systems in the Grid," *IEEE Trans. Sustain. Energy*, vol.5, no.4, pp.1204-1212, Oct. 2014.

[14] Lu, X.; Sun, K.; Guerrero, J.M.; Vasquez, J.C.; Huang, L., "State-of-Charge Balance Using Adaptive Droop Control for Distributed Energy Storage Systems in DC Microgrid Applications," *IEEE Trans. Ind. Electron.*, vol.61, no.6, pp.2804-2815, June 2014.

[15] Chung-Ming Young; Neng-Yi Chu; Liang-Rui Chen; Yu-Chih Hsiao; Chia-Zer Li, "A Single-Phase Multilevel Inverter With Battery Balancing," *IEEE Trans. Ind. Electron.*, vol.60, no.5, pp.1972-1978, May 2013.

[16] Inthamoussou, F.A.; Pegueroles-Queralt, J.; Bianchi, F.D., "Control of a Supercapacitor Energy Storage System for Microgrid Applications," *IEEE Trans. Energy Convers.*, vol.28, no.3, pp.690-697, Sept. 2013.

[17] Bostrom, A.; von Jouanne, A.; Brekken, T.K.A.; Yokochi, A., "Supercapacitor energy storage systems for voltage and power flow stabilization," *in Proc. 1st IEEE Conf. on Technologies for Sustainability (SusTech)*, vol., no., pp.230-237, 1-2 Aug. 2013.

[18] Wandhare, R.G.; Agarwal, V., "Novel Stability Enhancing Control Strategy for Centralized PV-Grid Systems for Smart Grid Applications," *IEEE Trans. Smart Grid.*, vol.5, no.3, pp.1389-1396, May 2014.

[19] Kamel, R.M.; Chaouachi, A.; Nagasaka, K., "Three Control Strategies to Improve the Microgrid Transient Dynamic Response During Isolated Mode: A Comparative Study," *IEEE Trans. Ind. Electron.*, vol.60, no.4, pp.1314-1322, April 2013.

[20] Massing, J.R.; Stefanello, M.; Grundling, H.A.; Pinheiro, H., "Adaptive Current Control for Grid-Connected Converters With LCL Filter," *IEEE Trans. Ind. Electron.*, vol.59, no.12, pp.4681-4693, Dec. 2012.

[21] Mohamed, Y. A -R I, "Mitigation of Converter-Grid Resonance, Grid-Induced Distortion, and Parametric Instabilities in Converter-Based Distributed Generation," *IEEE Trans. Power Electron.*, vol.26, no.3, pp.983-996, March 2011.

[22] Krommydas, K.F.; Alexandridis, A.T., "Modular Control Design and Stability Analysis of Isolated PV-Source/Battery-Storage Distributed Generation Systems," *IEEE J. Emerg. Sel. Topics Circuits Syst*, vol.5, no.3, pp. 372-382, 2015.

[23] Debnath, S.; Qin, J.; Saeedifard, M., "Control and Stability Analysis of Modular Multilevel Converter under Low-frequency Operation," *IEEE Trans. Ind. Electron.*, vol. 62, no.9, pp.5329-5339, 2015.

[24] Harnefors, L.; Antonopoulos, A.; Ilves, K.; Nee, H.-P., "Global Asymptotic Stability of Current-Controlled Modular Multilevel Converters," *IEEE Trans. Power Electron.*, vol.30, no.1, pp.249-258, Jan. 2015.

[25] Weiguo Lu; Shuang Lang; Luowei Zhou; Iu, H.H.-C.; Fernando, T., "Improvement of Stability and Power Factor in PCM Controlled Boost PFC Converter With Hybrid Dynamic Compensation," *IEEE Trans. Circuits Syst. I, Reg. Papers* , vol.62, no.1, pp.320,328, Jan. 2015

[26] Ting Qian; Wenkai Wu; Weidong Zhu, "Effect of Combined Output Capacitors for Stability of Buck Converters With Constant On-Time Control," *IEEE Trans. Ind. Electron.*, vol.60, no.12, pp.5585,5592, Dec. 2013

[27] Khaligh, A., "Realization of Parasitics in Stability of DC–DC Converters Loaded by Constant Power Loads in Advanced Multiconverter Automotive Systems," *IEEE Trans. Ind. Electron.*, vol.55, no.6, pp.2295-2305, June 2008.

[28] Wu Chen; Xinbo Ruan; Hong Yan; Tse, C.K., "DC/DC Conversion Systems Consisting of Multiple Converter Modules: Stability, Control, and Experimental Verifications," *IEEE Trans. Power Electron.*, vol.24, no.6, pp.1463-1474, June 2009

[29] Deshang Sha; Zhiqiang Guo; Tianmei Luo; Xiaozhong Liao, "A General Control Strategy for Input-Series–Output-Series Modular DC–DC Converters," *IEEE Trans. Power Electron.*, vol.29, no.7, pp.3766-3775, July 2014.

[30] K. J. A˚strom and T. H ¨ agglund, ¨ PID Controllers Theory: Design and Tuning" *Research Triangle Park, NC, USA: Instrum. Soc. Amer.*, 1995.

Nilanjan Mukherjee (S'12 – M'14) received Ph.D. degree in electronics engineering with a speciation in Power Electronics from the University of Aston, Birmingham, UK, in 2014.

He worked as a postdoctoral research associate in Aston University after completion his PhD. From 2009 to 2011, he was with the automotive industry working in the Engineering Research Centre (ERC) of Tata Motors Ltd. Pune, India. He was involved in power converter control in battery super-capacitor integration in Electric Vehicle drive train. He is currently with the school of electronic, electrical and systems engineering at the University of Birmingham, UK as a postdoctoral research fellow in Power Electronics.

He has been involved in multiple research projects from the research council and industries in the UK. He is the member of IEEE and IEEE industrial electronics society. He is also actively engaged in reviewing committee in various leading IEEE/IET conferences and journals such as, *IEEE transactions on Power Electronics*, *IEEE transactions on Industrial Electronics*, *IET Power Electronics* and so on. His main research area includes the role of power electronics in interfacing energy storage elements, energy management and hybrid energy systems. He is particularly interested in the design and development of new generation multi-modular/modular multilevel power converters, and advanced converter control methods for utility grid and machine drive systems.

Dani Strickland has a degree from Heriot Watt University and a PhD from Cambridge University, UK in Electrical Engineering. She has worked for Eon, Sheffield University, Rolls Royce Fuel Cells PLC and is currently employed at Aston University as a lecturer.

Her main research interests include the application of power electronics to power systems.